Pharm Res (2015) 32:2132–2143
DOI 10.1007/s11095-014-1604-z

RESEARCH PAPER

Graphene Oxide - Gelatin Nanohybrids as Functional Tools for Enhanced Carboplatin Activity in Neuroblastoma Cells

Sami Makharza • Orazio Vittorio • Giuseppe Cirillo • Steffen Oswald • Elizabeth Hinde • Maria Kavallaris • Bernd Büchner • Michael Mertig • Silke Hampel

Received: 26 May 2014 / Accepted: 10 December 2014 / Published online: 24 December 2014

ABSTRACT

Purpose Preparation of Nanographene oxide (NGO) - Gelatin hybrids for efficient treatment of Neuroblastoma.

Methods Nanohybrids were prepared *via* non-covalent interactions. Spectroscopic tools have been used to discriminate the chemical states of NGO prior and after gelatin coating, with UV visible spectroscopy revealing the maximum binding capacity of gelatin to NGO. Raman and X-ray photoelectron spectroscopy (XPS) demonstrated NGO and Gelatin_NGO nanohybrids through a new chemical environments produced after noncovalent interaction. Microscopic analyses, atomic force microscopy (AFM) and scanning electron microscopy (SEM) are used to estimate the thickness of samples and the lateral width in the nanoscale, respectively.

Results The cell viability assay validated Gelatin_NGO nanohybrids as a useful nanocarrier for Carboplatin (CP) release and delivery, without obvious signs of toxicity. The nano-sized NGO (200 nm and 300 nm) did not enable CP to kill the cancer cells efficiently, whilst the CP loaded Gel_NGO 100 nm resulted in a synergistic activity through increasing the local concentration of CP inside the cancer cells.

Conclusions The nanohybrids provoked high stability and dispersibility in physiological media, as well as enhanced the anticancer activity of the chemotherapy agent Carboplatin (CP) in human neuroblastoma cells.

KEY WORDS Anticancer activity · Gelatin · Nanohybrids · Nanographene oxide · Neuroblastoma

ABBREVIATIONS

AFM	Atomic force microscopy
CP	Carboplatin
CP@Gel	Gelatin loaded with carboplatin

Electronic supplementary material The online version of this article (doi:10.1007/s11095-014-1604-z) contains supplementary material, which is available to authorized users.

S. Makharza (✉) • G. Cirillo • S. Oswald • B. Büchner • S. Hampel
Leibniz Institute for Solid State and Materials Research Dresden
01171 Dresden, Germany
e-mail: Makharza.sami@gmail.com

G. Cirillo (✉)
Department of Pharmacy, Health and Nutritional Sciences
University of Calabria, 87036 Rende, (CS), Italy
e-mail: giuseppe.cirillo@unical.it

M. Mertig
Department of physical chemistry Technische Universität Dresden
01062 Dresden, Germany

E. Hinde • M. Kavallaris
ARC Centre of Excellence in Advanced Molecular Imaging
University of New South Wales, Sydney, Australia

O. Vittorio • M. Kavallaris
Children's Cancer Institute Australia, Lowy Cancer Research Centre
University of New South Wales, NSW Sydney, Australia

B. Büchner
Department of Physics, 01062
Technische Universität Dresden, Dresden, Germany

O. Vittorio • E. Hinde • M. Kavallaris
Australian Centre for NanoMedicine, University of New South Wales
NSW Sydney, Australia

M. Mertig
Kurt Schwabe Institute for Sensor Technology, 04736 Waldheim,
Germany

CP@Gel_NGO	Gelatin coated Nanographene oxide loaded with Carboplatin
CP@NGO	Nanographene oxide loaded with Carboplatin
CPT	Camptothecin
DMEM	Dulbecco's modified eagle medium
DOX	Doxorubicin
EDAX	Energy dispersive X-ray analysis
FBS	Fetal bovine serum
FWHM	Full width at half maximum
Gel	Gelatin
Gel_NGO	Gelatin coated nanographene oxide
GNS	Graphene nanosheets
GO	Graphene oxide
hMSCs	Human mesenchymal stem cells
IMR-32	Human neuroblastoma cells
LE	Loading efficiency
NGO	Nanographene oxide
PAMAM	Polyamidoamide
PBS	Phosphate buffered saline
PEG	Polyethylene glycol
Rho	Rhodamine B
Rho@Gel_NGO	Gelatin coated nanographene oxide loaded with rhodamine B
RT	Room temperature
SD	Standard deviation
SEM	Scanning electron microscope
SN-38	7-ethyl-10-hydroxycamptothecin
XPS	X-ray photoelectron spectroscopy

INTRODUCTION

Graphene is a one-atom thick of ordinary carbon atoms tightly packed into a two dimensional honeycomb like structure with unique, desirable, and outstanding physical and chemical properties. It was reported for the first time in 2004 and awarded Nobel Prize in physics in 2010 [1, 2]. Owning to its sp^2 hybrid structure and high surface area, graphene can be covalently decorated with oxygen containing functional groups and distorted to graphene oxide (GO). The functional groups (epoxy, hydroxyl, and carboxyl) alter the hybridization of graphene to sp^3 and distributed randomly onto the basal plane and edges. GO layers have a combination of sp^2 and sp^3 carbon atoms making it hydrophilic depending on the oxidation reaction conditions. The different hybridization - sp^2 and sp^3 - allows GO sheets to be functionalized with a wide range of molecules *via* covalent and/or noncovalent approaches [3–5]. For biological purposes, GO functionalization with organic molecules is crucial to optimize the stability in cell line media and to enhance the biocompatibility profiles. For the first time, Zhang et. Al, functionalized NGO with polyethylene glycol (PEG) for cellular imaging and anticancer drug delivery [6]. The chemical conjugation of PEG with NGO - COOH *via* covalent amide bond allows the obtained NGO - PEG system to be highly stable in aqueous media without any trace of agglomeration. *In vitro* biocompatibility experiments demonstrated an excellent cell viability response and endorsed it as a novel nanocarrier material for efficient drug delivery. Anticancer molecules, water soluble 7-ethyl-10-hydroxycamptothecin (SN-38) and camptothecin (CPT) were loaded on NGO - PEG *via* noncovalent interaction and revealed high stability in buffer solution.

The cell killing potency of NGO_PEG:SN-38 system was similar to those of free SN38 molecules, while was found to be higher than CPT - 11 (SN-38 prodrug) [7]. NGO - PEG nanocarrier has revolutionized the field of cancer therapy, and different anticancer agents and/or biomolecules like doxorubicin (DOX) [7], ribonuclease A [8], Biotin [9], and Cyanine dye [7, 10] were efficiently loaded and tested. After Zhang report, several studies have been published reporting the NGO functionalization with different materials like heparin [11], dextran [12], DNA [13], chitosan [14], gelatin [15], zero generation-polyamidoamide [16], *etc.*

In our study, we selected gelatin as the coating element for NGO particles, since this polypeptide chain exhibits excellent biocompatibility, biodegradability, and no cytotoxicity, and it is widely explored as a functional material for pharmaceutical and medical applications [15, 17, 18]. Gelatin functionalized graphene nanosheets composite (GNS - gelatin) revealed exceptional biocompatibility and physiological stability. Their cytotoxicity evaluation showed biocompatibility up to 200 μg/ml, and after DOX loading, high toxicity against human breast cancer cells was recorded, proving that GNS - gelatin can be considered an innovative and effective nano carrier in biomedical studies [19].

Here, we investigated the NGO coated gelatin (Gel_NGO), prepared *via* a fast and facile method, as a nanohybrid system for carboplatin delivery in an *in vitro* model consisting of Human neuroblastoma cells (IMR-32). Different spectroscopic and microscopic techniques have been used for size estimation and to improve functionalization, and the biological effects of drug and carrier extensively investigated. The ultimate aim of the study is to enhance the carboplatin efficiency by loading onto Gel_NGO nanohybrid.

The carrier is expected to increase the local concentration of the drug next to the cells, allowing drastic reduction of therapeutic dose, and thus the toxic side effects.

MATERIALS AND METHODS

Preparation of NGO and Size Reduction

NGO particles were synthesized by a modified hummers method [20]. Briefly, 1.0 g graphite (99.99%, −200 mesh,

Alfa Aesar) and 50.0 g NaCl (Sigma Aldrich, Germany) were ground for a few minutes using hand mortar and pestle. The ground graphite was suspended in distilled water to dissolve NaCl then removed by filtration. The collected graphite was mixed with 23 ml H_2SO_4 (96% w/w, Sigma Aldrich, Germany) overnight (H_2SO_4 intercalating graphite layers). Afterward, intercalated graphite suspension was placed in an ice bath to preserve the reaction temperature below 5°C (exothermic reaction). Subsequently, 3.0 g $KMnO_4$ (VWR, Germany) was added gradually with stirring to achieve graphite oxide. The resultant product was sonicated for 3 h and stirred for 30 min at 35°C and 45 min at 50°C respectively. Subsequently, 46 ml distilled water was poured to the mixture and stirred for 45 min at 98–105°C. Thereafter, the product was cooled down to room temperature, and then 40 ml distilled water and 10 ml 3% H_2O_2 (VWR, Germany) was added to reduce the residual permanganate and manganese dioxide to soluble manganese sulfate. The suspension was filtrated and washed three times with HCl (5% w/w Sigma Aldrich, Germany) and warm distilled water (40°C) to remove unfavorable materials. The resulting material was cracked in water under optimized conditions using a horn-tipped ultrasonic probe (BANDELIN ultrasonic, max. power of 25 – 60%) at 28 Watt for 2 hours, in order to reduce the dimensions (lateral width and thickness) of exfoliated GO sheets [16].

The NGO suspension was separated into different sizes *via* sucrose density gradient centrifugation [16, 21]. Briery, gradient sucrose solutions (20–60% w/v, Sigma Aldrich, Germany) were dropped gently into the bottom of centrifuged tube with exact volume. On the top of 20% sucrose, 335 ml NGO particles were added, the tube directly centrifuged under controlled conditions (5,880 g for 5 min) using BECKMAN COULTER, Allegra 64 R centrifuge. Along the tube, three visualized zones were produced - rinse thoroughly with distilled water to remove sucrose - and separated as three uniform sizes (NGO 100 nm, NGO 200 nm, and NGO 300 nm) for gelatin functionalization and carboplatin drug loading.

Preparation of Gel_NGO Nanohybrids

20 µL of Gelatin (Sigma-Aldrich, Germany) was added to a solution of NGO (1 mg ml^{-1}). The mixture was continuously stirred for 2 hours at RT and the resultant material, labeled Gel_NGO, was collected after centrifugation at 5,880 g for 2 min. To remove unbound gelatin, sample underwent three water dispersion/centrifugation cycles and the final material was dried overnight at 35°C.

Carboplatin Loading

In separate experiments, 20 µL of Carboplatin (1 mM, Pfizer, US) was mixed with 1 mg ml^{-1} NGO and Gel_NGO and stirred at RT for 2 hours. Thereafter, the products, labeled CP@NGO, CP@Gel_NGO, were collected after centrifugation at 5,880 g for 2 min and dried under vacuum in presence of P_2O_5 to constant weight. The loading efficiency percent (LE%) was calculated by UV–vis analysis of supernatant according to Eq. (1) :

$$LE(\%) = \frac{C_i - C_0}{C_i} \times 100 \quad (1)$$

where C_i and C_0 are the concentrations of drug in the loading solution and in the supernatant of centrifugation, respectively.

The calculated LE% values are listed in Table S1 (See SI).

Cell Culture and Viability Assay

Human Neuroblastoma cell line (IMR-32) were obtained from ATCC (CCL-127™) and Human Mesenchymal Stem Cells (hMSCs), which are primary and non-malignant cells, were obtained from Lonza. Cells were cultured in Dulbecco's Modified Eagle Medium (DMEM) supplemented with 10% fetal bovine serum (FBS, Lonza, Milan, Italy). 1% L-glutamate, and 1% penicillin / streptomycin (all chemicals purchased by Sigma-Aldrich). Cells were grown as a monolayer in a humidified atmosphere at 37°C and in 5% CO_2. NGO, CP@NGO, Gel_NGO, and CP@Gel_NGO were prepared for cell culture media (stock solution 1.0 mg ml^{-1} CP equivalent concentration) and stored at RT. Clinical grade carboplatin (1 mM, Pfizer, US) was acquired from the local pharmacy and stored at RT. Treatment effects on IMR-32 cell growth inhibition were measured on the basis of metabolic activity of cells using an Alamar blue assay and spectrophotometric analysis. Briefly, cells were plated in clear transparent 96-well plates at an optimized cell density of 5 10^4 cells.ml^{-1} (10^4 cells $well^{-1}$) 48 h prior to treatment.

Cells were then treated with either single compounds or their combinations and effects on cell growth assessed 24 h later.

Fluorescence Microscopy

Rhodamine B (Rho, Sigma-Aldrich, Germany) was loaded on Gel_NGO as follows: 0.01 mg of Rhodamine B was mixed with 50 mg Gel_NGO 100 and stirred at RT for 2 h. Thereafter, the product was purified from unloaded Rho by ultracentrifugation at 5,880 g for 2 min and dried under vacuum in presence of P_2O_5 to constant weight.

Cells were incubated for 6 h with Rho@Gel_NGO in complete cell culture media and subsequently washed three times in PBS and imaged. The microscopy measurements were performed on a Zeiss LSM780 Quasar laser scanning microscope, using a 40X water immersion objective 1.2 N.A.

(Zeiss, Germany). Rhodamine was excited with the 561 nm emission line of a diode pump solid state (DPSS) laser. Fluorescence was detected between 592–696 nm. A z stack of the fluorescence signal was acquired with an interval width of 0.55 μm and superimposed over the transmission image. The pinhole was set to 1 Airy Unit.

Morphology and Structure Characterization

Scanning Electron Microscope (SEM) images were obtained using a FEI, NOVA NanoSEM 200 with an acceleration voltage of 15 kV. Atomic Force Microscopy (AFM) images were acquired using Digital Instruments Veeco, NanoScope IIIa, operating in the tapping mode. The images were examined using WSxM software designed by Nanotech Electronica (Madrid, Spain) [22]. A Shimadzu UV–vis-NIR, MPC – 3100 Model, Dual beam spectrometer with PbS photomultiplier detector were used for UV – vis measurements. Raman spectra were recorded on a Thermo Scientific, DXR Smart Raman with an excitation laser wavelength of 532 nm.

X-ray photoelectron spectroscopy (XPS) measurements were carried out in an ultrahigh vacuum system ($<10^{-9}$ mbar) equipped with a hemispherical electron analyzer SPECS PHOIBOS 100. Photoelectrons in all XPS measurements were excited with non-monochromatic Mg Kα (1253.6 eV) radiation and analyzed with a constant pass energy of 15 eV. The X-ray source was run at a power of 300 watts.

Statistical Analysis

In cell viability assays, three independent experiments were performed in quadruplicate. The statistical values were expressed as means and the standard deviation (SD) was taken as the error. Statistical significance was assessed by one-way analysis of variance followed by post-hoc comparison test (Tukey's test). Significance was set at $p<0.01$.

RESULTS AND DISCUSSION

Synthesis, Characterization, and Functionalization of NGO

Pristine graphite oxide sonicated and centrifuged under typical conditions produced three samples of NGO particles named as L1, L2, and L3. An elemental micro-analysis (EDAX -Energy Dispersive X-ray analysis) revealed the presence of carbon and oxygen atoms without contaminations (see Figure S1 in the SI). The statistical analysis of the three layers discloses three sizes of NGO particles at 100 nm, 200 nm, and 300 nm respectively. The functional groups of exfoliated NGO particles are able to coordinate with the non-polar amino acid chains of gelatin *via* non-covalent interactions (Fig. 1), such as van der Waal, H - bonding, hydrophobic - hydrophobic, electrostatic, steric exclusion, *etc.* [15, 18]. The terminal amine NH_2 group in gelatin macromolecule is an electron donating group, driving electrons toward nucleophilic ring opening reaction [4]. CP, an anticancer drug agent particularly used for solid tumors, was loaded onto NGO sheets through non-covalent incorporation [16].

Figure 2 (a–c) exhibit SEM images of the three different sized NGO samples, in panel d, the statistical data of about 250 pristine NGO particles of the three samples revealed the lateral width at 100 nm, 200 nm, and 300 nm, respectively. Figure 3 (a–c) show AFM images of the three different sized NGO samples (the thickness of selected particle is shown below each image). The statistical analysis of about 250 particles of the three samples confirmed the thickness of pristine NGO particles as appeared in Fig. 3 panel g. The thickness for all samples is approximately 3.4 nm and the number of NGO sheets is ca. 6 (assuming an interlayer distance of 0.7 nm) [23]. Fig. 3 (d–f) represents Gel_NGO samples with clear change in particles thickness after coating by gelatin, the statistical data revealed that the thickness of coated NGO samples increased up to 12 nm (Fig. 3 panel h). The clear difference in images contrast - compering with pristine NGO samples - could be considered as another evidence for effective gelatin interaction.

UV Visible Spectroscopy

UV visible spectroscopy was used to estimate the amount of gelatin coating NGO particles [15]. Initially, standard gelatin solutions 2.0, 1.0, 0.8, 0.6, 0.5, 0.4, 0.3, 0.2 and 0.1 mg ml^{-1} were prepared in distilled water, followed by stirring at 40°C for complete dissolution. The absorbance of gelatin solutions were recorded (Fig. 4a, inset figure represents the calibration curve of gelatin for binding capacity calculation). 10 mg ml^{-1} NGO solution was allowed to react with gelatin at different concentrations at 40°C with stirring for 2 hours. As reported in the experimental section, the final product, labelled Gel_NGO, underwent three water dispersion/centrifugation cycles in order to remove unbound gelatin. Unbound gelatin was collected and metered to exact volume for binding capacity calculation. The binding capacity (q) can be estimated by the following equation (2).

$$q = \left[\frac{(C_0 - C_e)}{m}\right] \times V \tag{2}$$

Where q (mg mg^{-1}) is the amount of gelatin bound onto NGO, C_0 (mg ml^{-1}) the initial gelatin concentration, and C_e

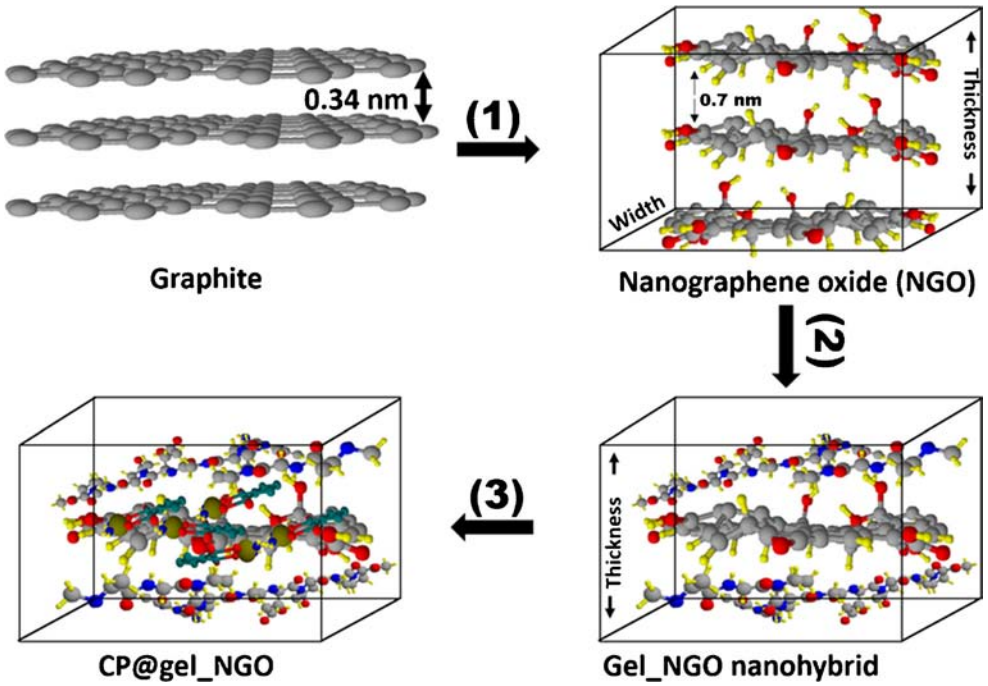

Fig. 1 Schematic illustration of CP@Gel_NGO preparation: (1) Chemical oxidation exfoliation reaction and size reduction, (2) coating by gelatin, and (3) CP loading

the concentration of unbound gelatin at equilibrium (estimated from the calibration curve of gelatin standard solution presented in Fig. 4a), V is the total volume of mixture (10 ml) and m is the mass of NGO (10 mg). As shown in Fig. 4b, the maximum capacity of gelatin to NGO is 4/1 (*w*/*w*) (Table 1). A slight change appeared at different NGO sizes: NGO 100 nm consumed more gelatin molecules than NGO 200 nm and NGO 300 nm, and the result indicated that NGO 100 nm (with more edges) can have more efficiency to bind with gelatin molecules. The efficiency of coating (%) can be estimated by using the following Eq. (3).

$$\text{Coating Efficiency } (\%) = \frac{C_0 - C_e}{C_0} \times 100 \tag{3}$$

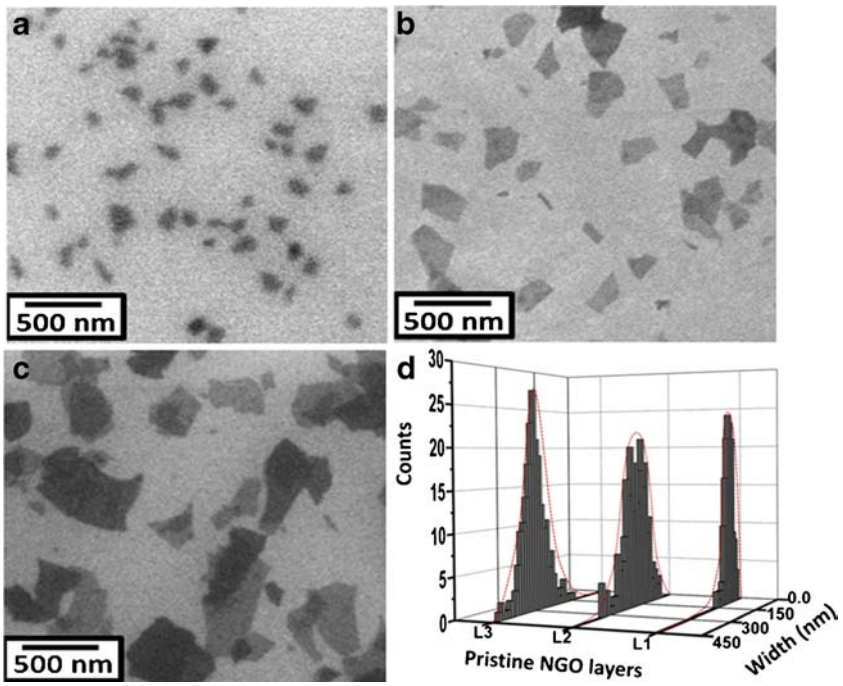

Fig. 2 (**a**–**c**) SEM images of pristine NGO 100 nm, 200 nm, and 300 nm respectively. (n.b.: the samples were deposited on silicon substrates for measurements. (**d**) Histogram of pristine NGO particles at different sizes deduced from SEM images

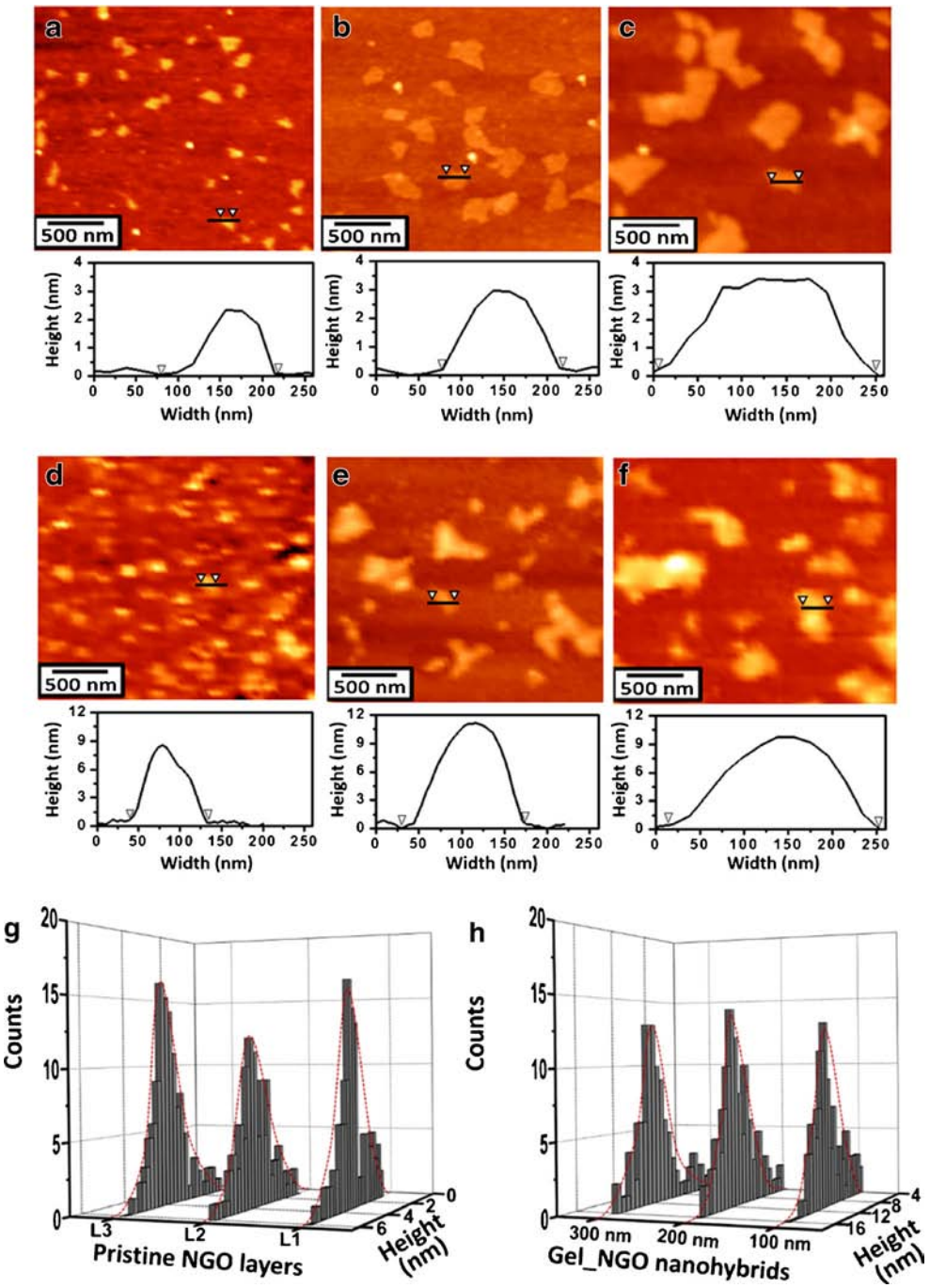

Fig. 3 (**a**–**c**) AFM images of pristine NGO 100 nm, 200 nm, and 300 nm respectively. (**d**–**f**) Gel_ NGO 100 nm, 200 nm, and 300 nm nanohybrids respectively (n.b.: samples were deposited on silicon substrates for measurements. (g and h) Histograms of the observed NGO particles at different sizes and Gel_ NGO nanohybrids respectively. The data deduced from AFM images

Raman Spectroscopy

Raman spectroscopy is used to study the vibrational regimes of graphite, pristine NGO and Gel_ NGO nanohybrids [24, 25]. Fig. 5a shows the characteristic bands of graphite at 1, 360, 1,578, and 2,705 cm^{-1}, corresponding to the D-, G-, and 2D-band respectively. The sp^2 carbon skeletal disorder induced D-band due to the presence of oxygen rich groups; this band is presumed to be a key for emphasizing the oxidation through the increment of band width and integrated intensity as shown in Fig. 5b. The G-band of graphite, sp^2 (C-C) bond appeared at 1,578 cm^{-1} is an interesting band by virtue of both its position and full width at half maximum (FWHM). NGO 100 nm revealed a significant change during oxidation in FWHM and intensity ratio I (D/G) to 0.9, as a result of oxygen incorporation [24]. The 2D-band at 2,705 cm^{-1} denoted the second order of D-band and the number of graphene layers, the functional groups on graphene basal plan

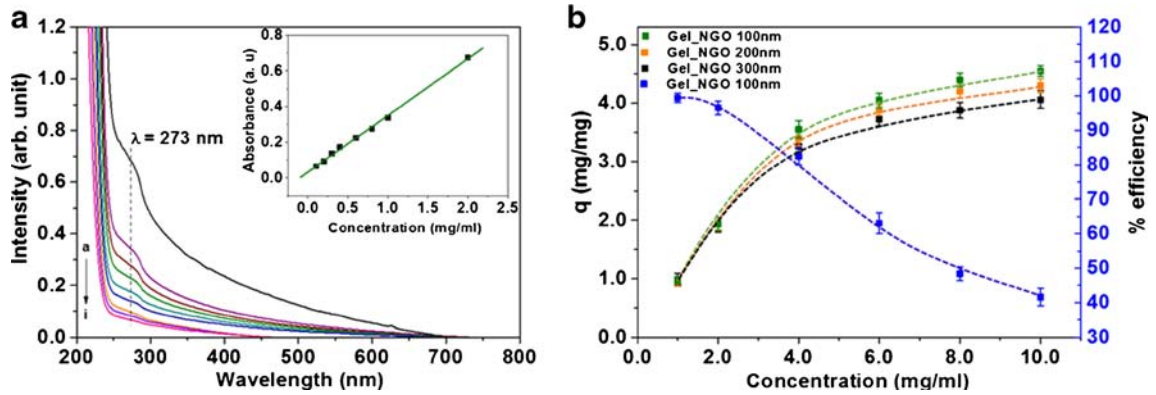

Fig. 4 **a** UV–vis absorption spectra of gelatin solutions at different concentrations (a -i): 2.0, 1.0, 0.8, 0.6, 0.5, 0.4, 0.3, 0.2, and 0.1 mg.ml^{-1} respectively (inset: calibration curve of gelatin) **b** Binding capacity of gelatin coated NGO particles at different sizes. Blue curve represents the percent efficiency of Gel NGO 100 nm

or edges reduced this band due to high structural disorder and exfoliation. Gel_NGO at different sizes show no considerable change in comparison with pristine NGO, however the Raman shift in the G-band position by ca. 25 cm^{-1} could be considered as an indication for functionalization (Fig. 5 (c–e)).

X-ray Photoelectron Spectroscopy

The chemical state of pristine NGO and Gel_NGO samples at all sizes were characterized using high resolution XPS. The C1s, O1s and N1s exhibit different components, indicating that these elements have different chemical environments (the peaks were fitted with Gaussian-Lorenzian mixed function). As shown in Fig. 6a, the C1s peaks appeared at 284.3, 285.6, 286.7, 287.3, and 288.5 eV are ascribed to sp^2 hybrids (C -C / C=C), hydroxyl (−OH), epoxy (C-O-C), carbonyl (C=O) and carboxyl (COOH) groups [16, 26]. The C1s spectra of CP@NGO 100 nm, Gel_NGO 100 nm, and CP@Gel_ NGO 100 nm revealed the same oxygen groups as shown in Fig. 6 (b–d). However NGO coated gelatin nanohybrid generates two prominent peaks for C-N and C (O)-N bonds at 286.4 and 287.2 eV, respectively, showing binding energies closed to those of C-OH and C=O [4, 27]. These finding are consistent with the N1s XPS spectra (Fig. 7a). As shown in Fig. 6 (e–h), the O1s XPS spectra of pristine and functionalized NGO were fitted to three main peaks around 531.2, 532.07, and 533.01 eV. These peaks are assigned to carboxyl, epoxide and hydroxyl groups and provide further information [16]. The C1s and O1s peak intensities of pristine NGO reduced drastically after coating by gelatin, as a result of deoxygenation. Figure 7b shows the Pt4f (7/2) and Pt4f (5/2) peaks originated from the immobilization of Platinum in the CP-loaded samples, confirming the non-covalent interactions between drug and with NGO [16, 28, 29]. The XPS spectra of NGO 200 nm, 100 nm, and functionalized materials exhibit analogous trends due to their structural similarity (see Figure S1-S5 in SI).

Biological Characterization

IMR-32 Human Neuroblastoma cells were selected as a model for evaluating the efficiency of the proposed nanohybrids to

Table 1 Binding capacity (q) of gelatin coated NGO particles and percent efficiency

Gel_NGO ratio (*w/w*)	q (mg mg^{-1}) *			Gel_NGO 100 nm (% efficiency)*
	Gel_ NGO 300 nm	Gel_ NGO 200 nm	Gel_ NGO 100 nm	
1:1	0.98	0.95	0.97	98.7
2:1	1.92	1.93	1.94	96.1
4:1	3.26	3.4	3.55	81.5
6:1	3.73	3.88	4.05	62.2
8:1	3.88	4.2	4.4	48.5
10:1	4.06	4.3	4.55	40.6

*data are expressed as mean. SD within 5%

q value and coating efficiency were calculated according to Eqs. 2 and 3, respectively

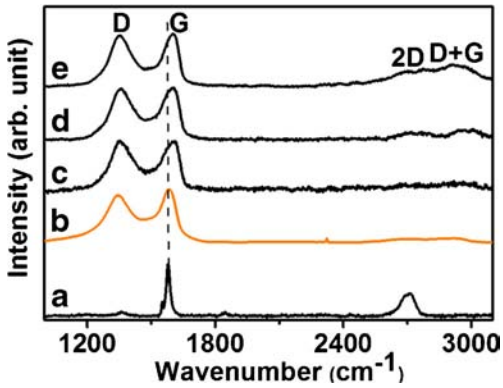

Fig. 5 Raman spectra of D, G, and 2D bands for (**a**) Graphite (**b**) pristine NGO 100 nm, and (**c**–**e**) Gel_NGO 100 nm, 200 nm, and 300 nm respectively

act as carriers for carboplatin, an anticancer drug widely used for the treatment of various cancer. Here, we explore the strategy of noncovalent modification by loading onto a hybrids nanocarrier, with the aim to enhance the anticancer efficiency of the drug.

CP was loaded with an efficiency of almost 100% for all samples (see Table 1 in SI), with Gel not significantly effecting the LE (%) at the selected concentration.

For the biological characterization, all the samples were tested at 5 μg ml^{-1} CP equivalent concentration, corresponding to a nanohybrid concentration of 25 μg/ml^{-1}. Any drug carrier and biomaterial proposed for use in biomedicine needs to strictly address the biocompatibility issues [30, 31]. The

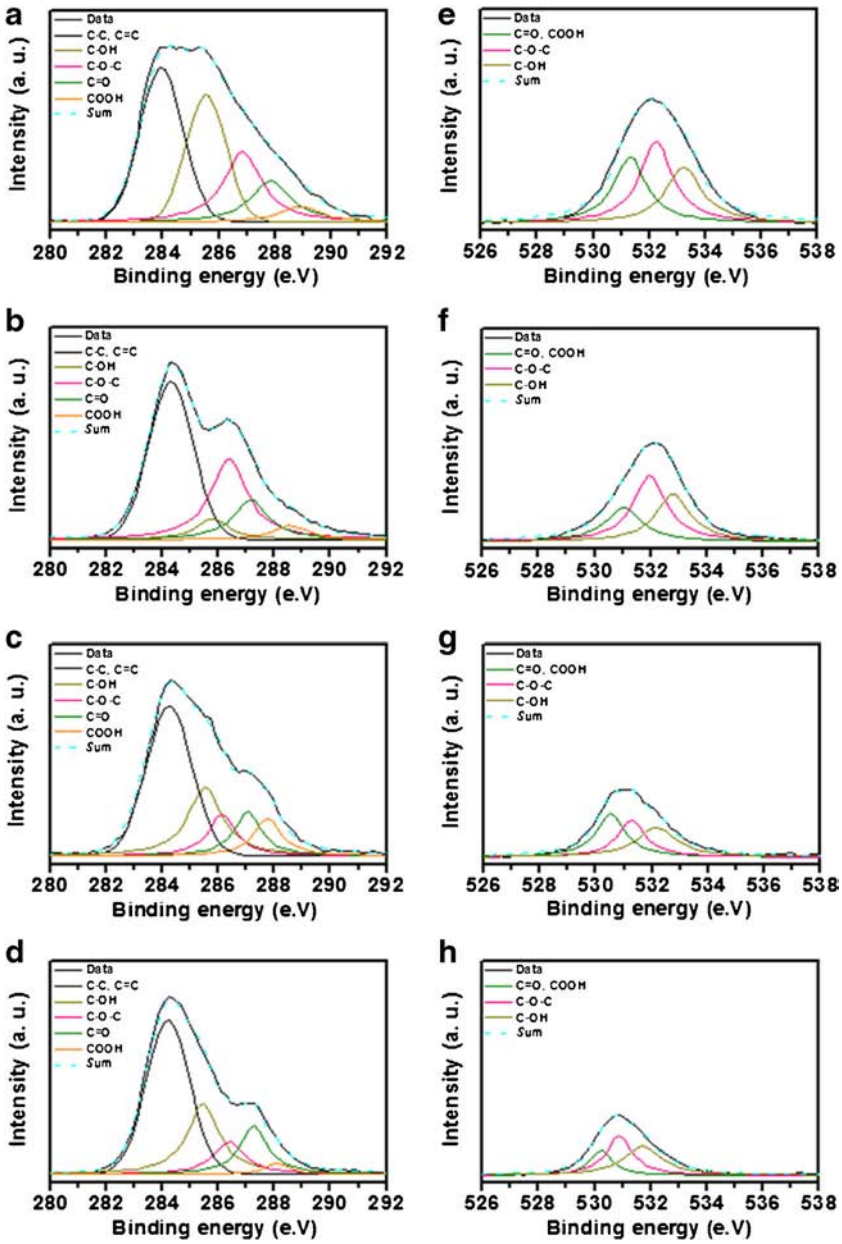

Fig. 6 C1s XPS spectra of NGO 100 nm (**a**) CP@NGO (**b**), Gel_NGO (**c**), and CP@Gel_NGO (**d**). O1s XPS spectra of NGO 100 nm (**e**), CP@NGO (**f**), Gel_NGO (**g**), and CP@Gel_NGO (**h**). All XPS data normalized at C - C peak position

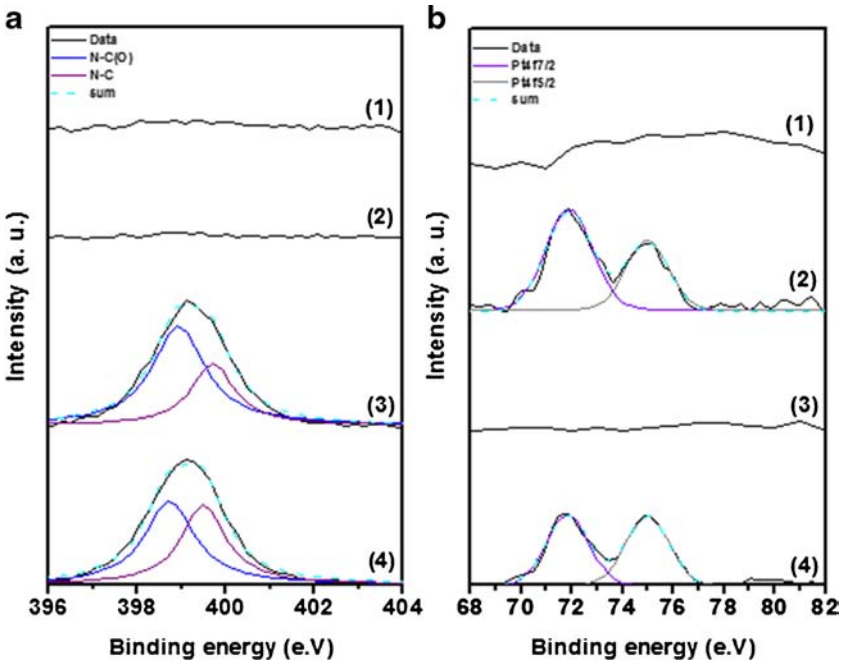

Fig. 7 (a: 1–4) N1s XPS spectra of pristine NGO 100 nm, CP@NGO, Gel_NGO, and CP@Gel_NGO respectively. (b: 1–4) Pt4f XPS spectra of pristine NGO 100 nm, CP@NGO, Gel_NGO, and CP@Gel_NGO, respectively

absence of any trace of toxic effect on non-malignant cells is the ideal behavior for biomaterials, and in this work we used hMSCs as an effective *in vitro* model for healthy cells, since their metabolic pathways confers them high susceptibility to foreign compounds and biomaterials [32, 33]. In our previous work [16], the activity of NGO on hMSCs at a concentration of 100 μg ml^{-1} was analyzed: the results showed a very high toxicity of the pristine NGO, and even at the concentration tested here (25 μg ml^{-1}), a cell viability value lower of ca. 30% is recorded, highlighting the need to functionalize the NGO surface before any kind of biological application (Fig. 8a). The toxicity results from both the generation of oxygen reactive species and the physical stress associated with the interaction of lipid cell membranes [34].

The suitability of the proposed strategy of the NGO functionalization with Gel was proven when considering the recorded biocompatibility of the Gel_NGO samples. Interestingly, as shown in Fig. 9, Gel is able to reduce the toxicity of all sized NGO due to the formation of a protein shell around the nanoparticles, allowing an easier NGO dispersion and preventing any kind of damage on the cell surface. The possibility to greatly increase the biocompatibility of any sized NGO by Gel coating is a key advantage when compared with the previously developed Polyamidoamide (PAMAM) functionalization [16], where a significant reduction of toxicity was recorded only for lower sized samples. This could be related to the high molecular weight of the protein, allowing a more efficient NGO coating, and thus a considerable reduction of toxic reactions on the cell surface. As expected, Gel alone did not affect the cell viability, while it was found to reduce the activity of CP. The CP efficiency is reduced by almost 50%, since it moves from 41 to 62% for CP and CP@Gel, respectively (Fig. 8b). When considering the activity of the CP@Gel_ NGO samples, the strong dependency between the efficiency and the size of the carriers is clearly evident. Gel_NGO 300 and Gel_NGO 200 were found to

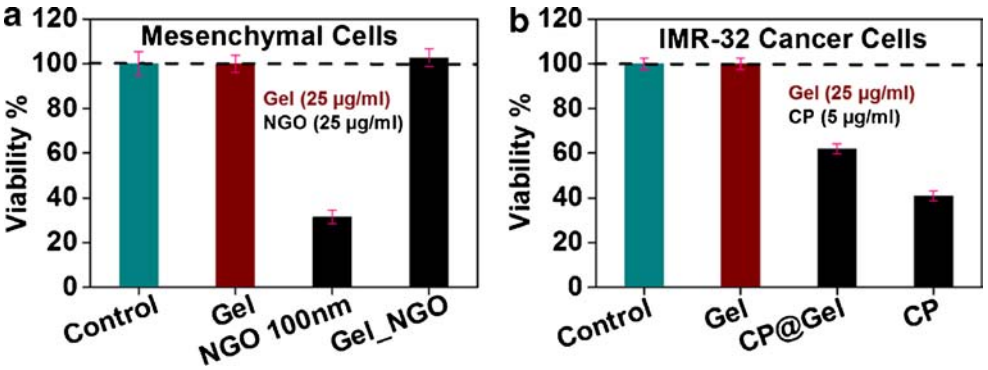

Fig. 8 The Cell viability of hMSCs (**a**) and IMR 32 cells (**b**) after 24 h of incubation

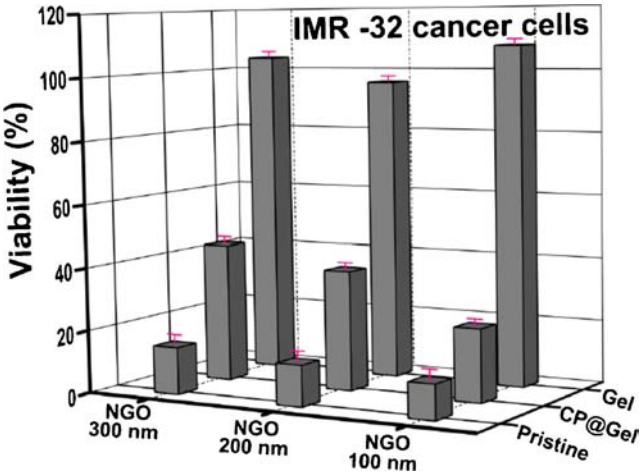

Fig. 9 Cell viability of NGO nanohybrids loaded CP

do not significantly modify the drug activity, as assessed by the recorded cell viability close to that of the free form of the drug. Gel_NGO 100 denotes a completely different behavior, since in this case the activity of the CP is almost doubled, with a cell viability of 41 and 23%, for CP and CP@Gel_NGO 100, respectively. The size dependency of the carrier efficiency is strictly related to their ability to interact with cells, and this is in agreement with data in literature showing that lower sized NGO are able to strongly interact with the cell environment with a more efficient delivery of the hosted drug.

The complex interactions between nanomaterial and cells have been reviewed extensively in the literature in view of the potential use of nanoparticles as intracellular transporters [35]. These interactions include electrostatic adsorption of nanoparticles on to the cell membrane, followed by their internalization into the cells. Many mechanism have been proposed, *e.g.*, penetration through an energy-independent non-endocytotic pathway, endocytosis and phagocytosis [36]. In our study, optical microscopy shows some black spots on the cells incubated with the NGO (Fig. 10b). Furthermore, cells treated only for 6 h with NGO, washed three times with PBS, detached and pelleted by centrifugation show a black pellet, typical color of the NGO (Figure S6 in SI). On the other side, cells treated with the free Gelatin, washed in PBS and centrifuged show a normal white pellet.

To further characterize the biological behavior of Gel_NGO 100, suitable confocal microscopy experiments were performed. At first, we demonstrated that marker remained absorbed onto the surface of graphene nanohybrids until the end of biological experiments by suitable releasing experiments (data not shown) [37]; then IMR-32 cells were incubated with Rhodamine B loaded Gel_NGO 100 for 6 h and imaged (Fig. 11). Our pictures clearly showed that the NGO were able to be internalized by the cells. Moreover it is interesting that the presence of the NGO was detected only in the cytoplasm, and not in the nucleus, after 6 h of incubation.

The whole of the biological data denote the ability of the carrier to increase the local concentration of the drug inside the cell environment, thus resulting in enhanced activity. Studies related to targeting behavior are expected to further increase the clinical applicability of the proposed nanohybrid, since the presence of Gel offers functional groups (*e.g.* heteroatoms in the protein side chain) able to undergo different types of chemical functionalization with targeting units. Anyway, the key result of the present study is the characterization of the synergistic activity between Gel_NGO 100 and CP, which is of tremendous importance when considering potential clinical applications, since it is possible to dramatically reduce the drug doses, with the advantages of reducing systemic side effects. Furthermore, a potential enhancement of the drug desired properties such as increased water solubility, cellular uptake, and targeted delivery, can be obtained. In conclusion, it can be hypothesized the development of a combination therapeutic protocol involving the use of the proposed nanohybrid carrier.

CONCLUSION

Biocompatible NGO coated gelatin nanohybrids could be used as an operational CP delivery vehicles for the treatment

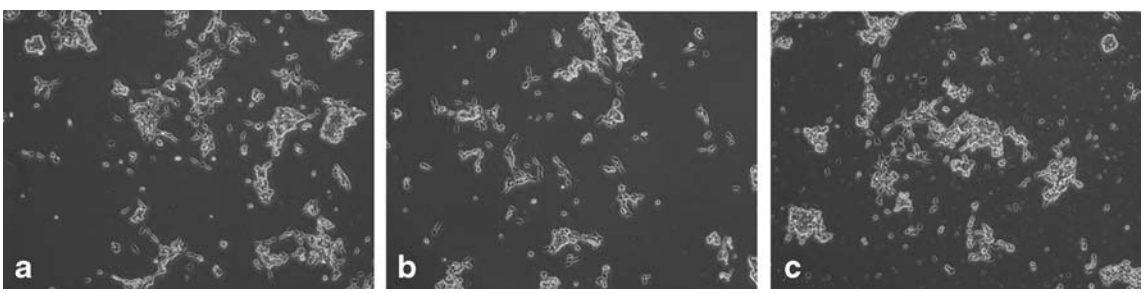

Fig. 10 Optical microscopy images of IMR 32 cells (**a**) incubated for 6 h with Gel (**b**) and Gel_NGO (**c**)

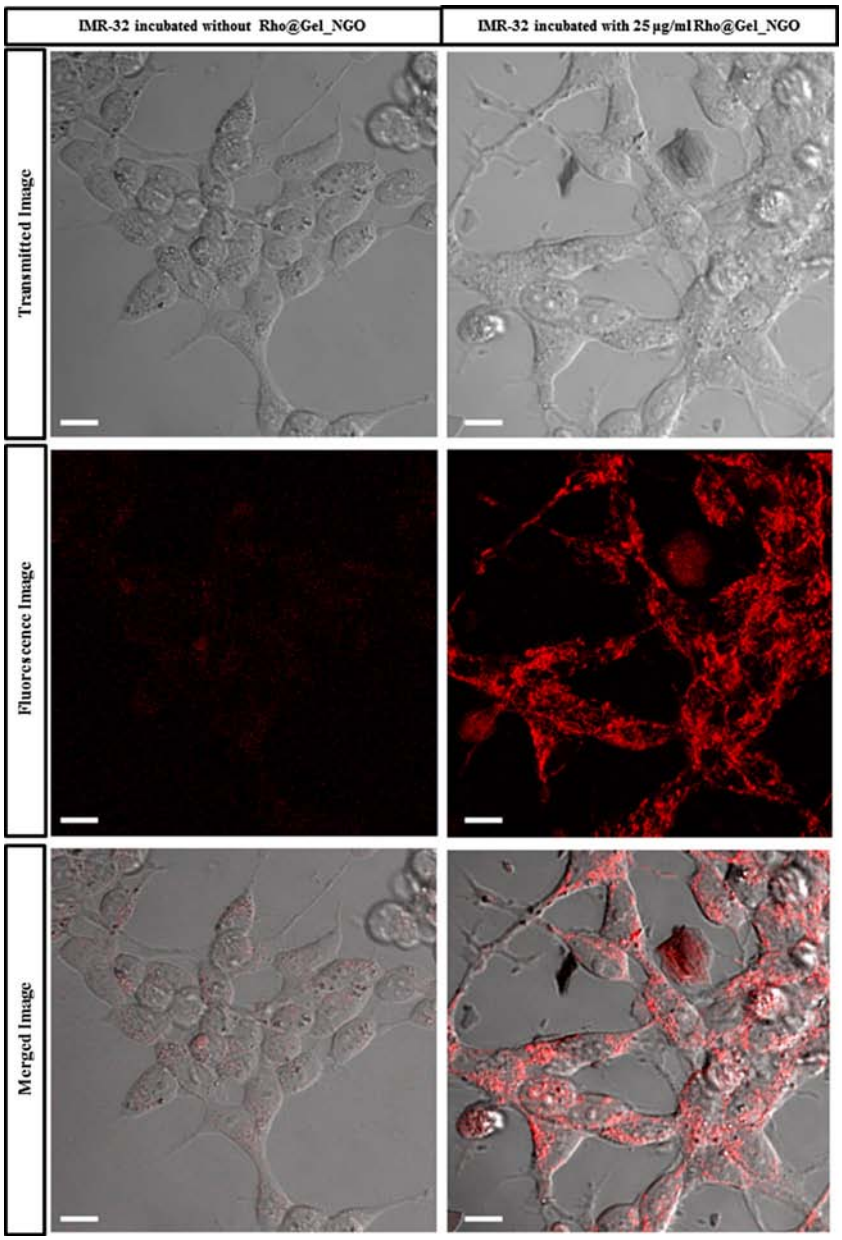

Fig. 11 Fluorescence microscopy images of IMR 32 cells incubated for 6 h with Gel_NGO. Scale bar 10 μm

of IMR-32 human Neuroblastoma Cells. The interaction of NGO particles with Gel has been obtained through noncovalent chemistry. The lower sized NGO 100 nm coated with gelatin exhibits excellent stability and biocompatibility in cell culture media according to their potency to interact with cellular membrane. A synergistic activity between CP and carrier was recorded, as suggested by the enhanced efficiency in killing cancer cells. Interestingly, the cell viability was not affected by Gel_NGO, confirming that the recorded anticancer activity is related to an increased local concentration of the drug within the cells environment, thus resulting in enhanced activity. Further investigation should be done to this regard, but the data reported have evidenced a very promising starting point for further research by chemists, nanotechnologists, biologists and oncologists.

ACKNOWLEDGMENTS AND DISCLOSURES

S.M. thanks the DAAD and Al-Quds University. G.C. thanks the financial support of Regional Operative Program (ROP) Calabria ESF 2007/2013IV Axis Human Capital Operative Objective M2 Action D.5. NHMRC Established Career Fellowship Award (M.K.). M.M. acknowledges financial support from the Excellence Cluster for Advancing Electronics Dresden (contract EXC1056). We thank Steffi Kaschube, Marco

Rosenkranz, David Kunhard, and Alexander Schubert for lab assistance. O.V. thanks the Cancer Institute New South Wales Fellowship.

REFERENCES

1. Novoselov KS, Jiang D, Schedin F, Booth TJ, Khotkevich VV, Morozov SV, *et al.* Two-dimensional atomic crystals. Proc Natl Acad Sci U S A. 2005;102:10451–3.
2. Novoselov KS, Geim AK, Morozov SV, Jiang D, Zhang Y, Dubonos SV, *et al.* Electric field effect in atomically thin carbon films. Science. 2004;306:666–9.
3. Makharza S, Cirillo G, Bachmatiuk A, Ibrahim I, Ioannides N, Trzebicka B, *et al.* Graphene oxide-based drug delivery vehicles: functionalization, characterization, and cytotoxicity evaluation. J Nanoparticle Res. 2013;15:2099–124.
4. Georgakilas V, Otyepka M, Bourlinos AB, Chandra V, Kim N, Kemp KC, *et al.* Functionalization of graphene: covalent and non-covalent approaches, derivatives and applications. Chem Rev. 2012;112:6156–214.
5. Wang Y, Li Z, Wang J, Li J, Lin Y. Graphene and graphene oxide: biofunctionalization and applications in biotechnology. Trends Biotechnol. 2011;29:205–12.
6. Zhang W, Guo Z, Huang D, Liu Z, Guo X, Zhong H. Synergistic effect of chemo-photothermal therapy using PEGylated graphene oxide. Biomaterials. 2011;32:8555–61.
7. Liu Z, Robinson JT, Sun X, Dai H. PEGylated nano-graphene oxide for delivery of water insoluble cancer drugs. J Am Chem Soc. 2008;130:10876–7.
8. Shen H, Liu M, He H, Zhang L, Huang J, Chong Y, *et al.* PEGylated graphene oxide-mediated protein delivery for cell function regulation. ACS Appl Mater Interfaces. 2012;4:6317–23.
9. Tan X, Feng L, Zhang J, Yang K, Zhang S, Liu Z, *et al.* Functionalization of graphene oxide generates a unique interface for selective serum protein interactions. ACS Appl Mater Interfaces. 2013;5:1370–7.
10. Yang K, Zhang S, Zhang G, Sun X, Lee S-T, Liu Z. Graphene in mice: ultrahigh in vivo tumor uptake and efficient photothermal therapy. Nano Lett. 2010;10:3318–23.
11. Lee DY, Khatun Z, Lee J-H, Lee Y-K, In I. Blood compatible graphene/heparin conjugate through noncovalent chemistry. Biomacromolecules. 2011;12:336–41.
12. Zhang S, Yang K, Feng L, Liu Z. In vitro and in vivo behaviors of dextran functionalized graphene. Carbon. 2011;49:4040–9.
13. Tang L, Wang Y, Liu Y, Li J. DNA-directed self-assembly of graphene oxide with applications to ultrasensitive oligonucleotide assay. 2011;3817–22.
14. Bao H, Pan Y, Ping Y, Sahoo NG, Wu T, Li L, *et al.* Chitosan-functionalized graphene oxide as a nanocarrier for drug and gene delivery. Small. 2011;7:1569–78.
15. An J, Gou Y, Yang C, Hu F, Wang C. Synthesis of a biocompatible gelatin functionalized graphene nanosheets and its application for drug delivery. Mater Sci Eng C. 2013;33:2827–37.
16. Makharza S, Cirillo G, Bachmatiuk A, Vittorio O, Mendes RG, Oswald S, *et al.* Size-dependent nanographene oxide as a platform for efficient carboplatin release. J Mater Chem B. 2013;1:6107–14.
17. Cirillo G, Vittorio O, Hampel S, Spizzirri UG, Picci N, Iemma F. Incorporation of carbon nanotubes into a gelatin-catechin conjugate: innovative approach for the preparation of anticancer materials. Int J Pharm. 2013;446:176–82.
18. Zheng W, Zheng YF. Gelatin-functionalized carbon nanotubes for the bioelectrochemistry of hemoglobin. Electrochem Commun. 2007;9:1619–23.
19. Liu K, Zhang JJ, Cheng FF, Zheng TT, Wang C, Zhu JJ. Green and facile synthesis of highly biocompatible graphene nanosheets and its application for cellular imaging and drug delivery. J Mater Chem. 2011;21:12034–40.
20. Hummers WS, Offeman RE. Preparation of graphitic oxide. J Am Chem Soc. 1958;80:1339–9.
21. Sun X, Luo D, Liu J, Evans DG. Monodisperse chemically modified graphene obtained by density gradient ultracentrifugal rate separation. ACS Nano. 2010;4:3381–9.
22. Horcas I, Fernández R, Gómez-Rodríguez JM, Colchero J, Gómez-Herrero J, Baro AM. WSXM: a software for scanning probe microscopy and a tool for nanotechnology. Rev Sci Instrum. 2007;78:013705–8.
23. Schniepp HC, Li JL, McAllister MJ, Sai H, Herrera-Alonso M, Adamson DH, *et al.* Functionalized single graphene sheets derived from splitting graphite oxide. J Phys Chem B. 2006;110:8535–9.
24. Kudin KN, Ozbas B, Schniepp HC, Prud'homme RK, Aksay IA, Car R. Raman spectra of graphite oxide and functionalized graphene sheets. Nano Lett. 2008;8:36–41.
25. Pimenta MA, Dresselhaus G, Dresselhaus MS, Cançado LG, Jorio A, Saito R. Studying disorder in graphite-based systems by Raman spectroscopy. Phys Chem Chem Phys. 2007;9:1276–91.
26. Haubner K, Murawski J, Olk P. The route to functional graphene oxide. ChemPhysChem. 2010;11:2131–9.
27. Yang H, Shan C, Li F, Han D, Zhang Q, Niu L. Covalent functionalization of polydisperse chemically-converted graphene sheets with amine-terminated ionic liquid. Chem. Commun. 2009;3880–2.
28. Biesinger MC, Payne BP, Grosvenor AP, Lau LWM, Gerson AR, Smart RSC. Resolving surface chemical states in XPS analysis of first row transition metals, oxides and hydroxides: Cr, Mn, Fe, Co and Ni. Appl Surf Sci. 2011;257:2717–30.
29. Yi H-B, Lee HM, Kim KS. Interaction of benzene with transition metal cations: theoretical study of structures, energies, and IR spectra. J Chem Theory Comput. 2009;5:1709–17.
30. Spizzirri UG, Hampel S, Cirillo G, Nicoletta FP, Hassan A, Vittorio O, *et al.* Spherical gelatin/CNTs hybrid microgels as electro-responsive drug delivery systems. Int J Pharm. 2013;448:115–22.
31. Yue H, Wei W, Yue Z, Wang B, Luo N, Gao Y, *et al.* The role of the lateral dimension of graphene oxide in the regulation of cellular responses. Biomaterials. 2012;33:4013–21.
32. Vittorio O, Cirillo G, Iemma F, Di Turi G, Jacchetti E, Curcio M, *et al.* Dextran-catechin conjugate: a potential treatment against the pancreatic ductal adenocarcinoma. Pharm Res. 2012;29:2601–14.
33. Akhavan O, Ghaderi E, Akhavan A. Size-dependent genotoxicity of graphene nanoplatelets in human stem cells. Biomaterials. 2012;33:8017–25.
34. Chng ELK, Sofer Z, Pumera M. Cytotoxicity profile of highly hydrogenated graphene. Chem Eur J. 2014;20:6366–73.
35. Ku SH, Lee M, Park CB. Carbon-based nanomaterials for tissue engineering. Adv Healthcare Mat. 2013;2:244–60.
36. Pryzhkova MV. Concise review: carbon nanotechnology: perspectives in stem cell research. Stem Cells Trans Med. 2013;2:376–83.
37. Musumeci T, Pellitteri R, Spatuzza M, Puglisi G. Nose-to-brain delivery: evaluation of polymeric nanoparticles on olfactory ensheathing cells uptake. J Pharm Sci. 2014;103:628–35.